Received: 12 April 2020 | Accepted: 29 July 2020

DOI: 10.1111/1365-2745.13485

Journal of Ecology | BRITISH ECOLOGICAL SOCIETY

RESEARCH ARTICLE

Trade-off between standing biomass and productivity in species-rich tropical forest: Evidence, explanations and implications

Takashi S. Kohyama[1] | Matthew D. Potts[2] | Tetsuo I. Kohyama[1] | Kaoru Niiyama[3] | Tze Leong Yao[4] | Stuart J. Davies[5] | Douglas Sheil[6]

[1]Faculty of Environmental Earth Science, Hokkaido University, Sapporo, Japan; [2]Department of Environmental Science, Policy, and Management, University of California, Berkeley, CA, USA; [3]Department of Forest Vegetation, Forestry and Forest Products Research Institute, Tsukuba, Japan; [4]Forestry and Environment Division, Forest Research Institute Malaysia, Kepong, Malaysia; [5]Center for Tropical Forest Science-Forest Global Earth Observatory, Smithsonian Tropical Research Institute, Washington, DC, USA and [6]Faculty of Environmental Sciences and Natural Resource Management, Norwegian University of Life Sciences, Ås, Norway

Correspondence
Takashi S. Kohyama
Email: kohyama@ees.hokudai.ac.jp

Funding information
Japan Society for the Promotion of Science, Grant/Award Number: 18H02504

Handling Editor: Gerhard Zotz

Abstract

1. Despite its broad implications for community structure and dynamics, we lack a clear understanding of how forest productivity is partitioned among tree species. As leaf mass per unit of standing biomass declines with tree size, species achieving larger stature should show lower relative productivity as compared to smaller stature species. However, many observations indicate large-stature species grow faster than small-stature species. In this study, we address this apparent paradox, and clarify interspecific trade-offs between turnover rates and maximum size in terms of forest-level productivity and biomass storage.
2. We examined data from the 1990 and 2000 surveys of the Pasoh 50-ha plot of Malaysian rain forest. In these data, individual stems ≥1 cm stem diameter (dbh) have been identified, marked, measured and mapped. We applied site-specific equations to estimate tree biomass from dbh. We estimated species-level productivity and loss rates that are less influenced by census interval-related effects and biases.
3. Among 390 abundant tree species, species with high stand-level biomass were predominantly those large-stature species where individuals could achieve large sizes. We found that relative (= per-species-biomass) productivity and loss rate, per-capita recruitment and mortality of species were all negatively correlated to species biomass and maximum size, but not to species abundance.
4. Large-stature species grew faster than small-stature species at the same tree sizes up to 36 cm dbh. However, the relative growth of large species at their maximum size markedly declined. As a result, tree-level relative growth at maximum size and species-level relative productivity decreased with species-level biomass.

5. Performing further analyses using smaller plots in four old-growth forests in Indonesia and Japan, we observed a similar interspecific negative relationship between relative productivity and biomass. We expect this phenomenon is widespread across species-rich forests.
6. *Synthesis*. How productivity is partitioned among species determines and reflects forest ecosystem functioning and species coexistence. Many species with low biomass and small maximum stem sizes disproportionally contribute to forest primary productivity, rapid recovery and resilience. In contrast, long-lived, high-biomass species contribute disproportionally to ecosystem stability and carbon storage. This complementarity reflects differentiation by adult stature among species.

KEYWORDS
adult stature, biodiversity, demography, ecosystem function, growth, mortality, plant population and community dynamics, species coexistence

1 | INTRODUCTION

The diversity of life histories found within mixed species communities influences coexistence and ecosystem properties (Falster, Brännström, Westoby, & Dieckmann, 2017; Hooper et al., 2005; Liang, Zhou, Tobin, McGuire, & Reich, 2015). Previous studies have found that net primary productivity is correlated with community species diversity at the level of forest stands (Chisholm et al., 2013; Jucker et al., 2016; Mori, 2018). However, it remains unclear how stand-level productivity is partitioned among co-occurring tree species with differing life histories.

Past studies of stand productivity have various shortcomings. Most have neglected spatial variation and differences among species (Kira & Shidei, 1967; Malhi et al., 2004; Phillips et al., 1998). When studies have examined interspecific variation, they have typically neglected stand-level processes and focused on selected, for example, common species (Condit, Sukumar, Hubbell, & Foster, 1998; Kohyama, Suzuki, Partomihardjo, Yamada, & Kubo, 2003; Poorter et al., 2008). Furthermore, conventional estimates of net primary production by tree growth (Clark et al., 2001; Kira & Shidei, 1967; Ohtsuka et al., 2005)—biomass gained through growth of surviving stems and by new recruits divided by the census interval—are problematic for a number of reasons including their inability to account for productivity during inter-census intervals (Malhi et al., 2004; Talbot et al., 2014). To remedy these shortcomings, we developed a method for estimating instantaneous rates of production and loss that is less impacted by census interval effects and biases (see Kohyama, Kohyama, & Sheil, 2019). In addition, by defining stand-level production as the sum of species-level production, biases due to ignoring interspecific heterogeneity are avoided. Using this new approach, we clarify how forest production is partitioned among tree species.

If the largest tree sizes in a population represent the population-level biomass, then a pattern similar to stand-level biomass distributions should arise (Bastin et al., 2018; Lutz et al., 2018; Slik et al., 2013): large-stature species have higher species biomass as compared to small-stature species. We further expected that the relative growth and mortality of individual trees at the species maximum size would represent species-level relative productivity and loss, respectively (Figure 1). Therefore, it is necessary to relate species-level biomass turnover to species demography as measured by tree-size dependent growth and mortality.

Species-level biomass turnover (i.e. per-biomass relative rate of production and loss) is either negatively, positively or not related to species biomass in a community. The negative turnover-biomass correlation could be expected from the following assumptions. The relative growth of individual forest trees generally decreases with increasing size in any species population (Iida et al., 2014; Kohyama, Potts, Kohyama, Abd Rahman, & Ashton, 2015). This trend likely

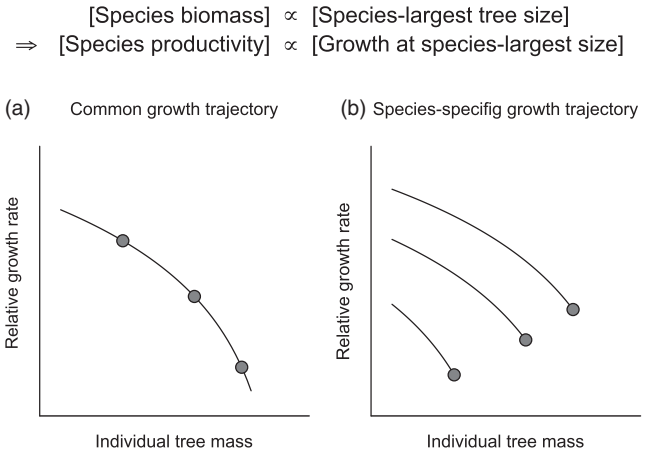

FIGURE 1 Assumed link between species-level biomass productivity, and size-dependent tree growth trajectory. Circles indicate species maximum individual tree values for large-, intermediate- and small-stature species. (a) Forest-wide decline of relative growth with tree size predicts a negative relationship between relative productivity and biomass. (b) Interspecific differentiation in growth curves may bring about an increasing relationship between relative productivity and biomass

reflects the reduced ratio of photosynthetic leaves, and thus available energy capture, in relation to total tree biomass (Enquist & Niklas, 2002; Poorter et al., 2012, 2015). Assuming that the decline of relative growth with tree size is similar among species with varied maximum sizes then large-stature species should show lower relative growth at maximum tree size and species-level relative productivity (Figure 1a). Tree mortality at maximum size and species-level relative loss would also be lower in large-stature species than in small-stature species (Iida et al., 2014; Kohyama et al., 2015). However, at the stand-scale, larger (and taller) trees capture a greater share of available light than smaller (and shorter) trees, which may compensate for the cost of achieving large tree size.

In reality, there is interspecific variation in size-dependent growth of trees. Observations in tropical forests suggest that species with larger stature typically grow faster, have lower mortality and recruit less frequently as compared to species with smaller stature (Iida et al., 2014; King, Davies, & Noor, 2006; King, Wright, & Connell, 2006; Kohyama et al., 2003, 2015; Lieberman, Lieberman, Hartshorn, & Peralta, 1985; Manokaran & Kochummen, 1987; Poorter et al., 2008; Rüger et al., 2018). Smaller stature species compensate for slow growth by maturing sooner and recruiting more frequently. Theoretically, lower mortality-to-growth ratios over a tree size range results in larger maximum tree sizes in stable populations (Kohyama et al., 2015). Sillett et al. (2010) and Stephenson et al. (2014) suggest that absolute (not relative) productivity of forest trees steadily increases with tree size; though the evidence remains ambiguous (Ligot et al., 2018; Sheil et al., 2017). In addition, mortality does not simply decline with tree size, but shows a minimum among mid-sized trees, with increasing rates of both smaller and larger stems (Coomes & Allen, 2007; Iida et al., 2014; King, Davies, et al., 2006; King, Wright, et al., 2006; Kohyama et al., 2015; Rüger, Huth, Hubbell, & Condit, 2011). We wish to examine how tree mortality at species maximum size relates to total species biomass. Therefore, it remains possible that species-level biomass turnover (relative productivity and loss) is positively related to species biomass (Figure 1b).

To guide our work, we propose the following four complementary hypotheses: (1) In a mixed-species stand, species that achieve large sizes (i.e. in which some individuals achieve large diameters and stature) have higher species–population biomass than smaller sized species (n.b. this is not a truism: it would be false if small-stature species were sufficiently common and large-stature species sufficiently rare), (2) species population-wide relative production rates are lower for higher biomass species; (3) low species-level relative productivity for high-biomass species is explained by large-stature species possessing a lower proportion of photosynthetic leaves to wood mass than small-stature species and (4) despite the fact that individual trees of large sized species grow faster than those of small sized species at equivalent individual stem sizes, marked reduction of tree-level relative growth at large tree sizes brings about lower species-level relative productivity for large-stature, high-biomass species.

To test these hypotheses, we examined data from the Pasoh 50-ha forest plot in Peninsular Malaysia. We estimated and compared the biomass turnover (productivity and loss) and abundance turnover (recruitment and mortality) of 390 co-occurring tree species. From repeated tree inventory data, we generated 'identity-free' data, in which we replaced the species identity and spatial position of a stem with another stem of similar diameter. Comparing results of observed and identity-free communities allowed us to disentangle species properties from effects of forest-wide tree size dependence. We also quantified stem size dependence of individual growth and mortality for every species, to relate biomass turnover by ontogeny and life history. We examined the generality of our results by analysing data from four other old-growth forests.

2 | MATERIALS AND METHODS

2.1 | Pasoh plot data

We used data from the 50-ha forest dynamics plot (2°59′N, 102°18′E) located in an intact lowland mixed dipterocarp forest in the Pasoh Forest Reserve, Negeri Sembilan, Peninsular Malaysia, where tree stems ≥1.0 cm in diameter at breast height (hereafter, dbh) have been identified, tagged and their dbh measured to the nearest 0.1 cm, since 1986 (Condit et al., 1999; Davies, Noor, LaFrankie, & Ashton, 2003; Manokaran & LaFrankie, 1990). We used data from two censuses (~1990 and ~2000). For individual trees, the time interval varied from 10.02 to 11.25 years. Biomass estimates were determined using allometric equations (Niiyama et al., 2010) calibrated using destructive sampling at Pasoh in 2004–2005; these equations estimate tree height (m), leaf mass and stem plus branch mass, and coarse root mass (Mg oven dry mass) from dbh (cm). We estimated leaf mass and above-ground mass (i.e. leaf mass plus stem–branch mass) of every tree in two censuses using these in situ equations. These equations disregard interspecific differences though we note that the allometries of tree height versus dbh in the Pasoh plot are not significantly different among the most abundant 200 tree species, and across maximum species sizes (Iida et al., 2011). We examined the effect of interspecific variation in stem wood density using the Global Wood Density Database (Zanne et al., 2009). Large declines in measured dbh between censuses, where the change in log dbh between the two censuses was smaller than −0.1 (or more than *c*. 10% reduction), were considered as the death of one stem and recruitment of a new stem by regrowth (Kohyama et al., 2015).

To disentangle the effects of species-specific demographic properties and response to local site conditions from effects of forest-wide average tree-size dependence, we generated an 'identity-free' dataset, in which demography is independent of species identity and location (Figure 2). To generate the identity-free data, we first sorted the trees in the observed data in order of their dbh in the 1990 census (tied values were randomized), and swapped species identity and location between every neighbouring pair of odd- and even-number trees in the sorted data, leaving other tree measures (dbh in two censuses and time interval) unchanged. By using this procedure, each identity-free 'species' population possesses a tree-size distribution similar to that observed, but growth, survival and

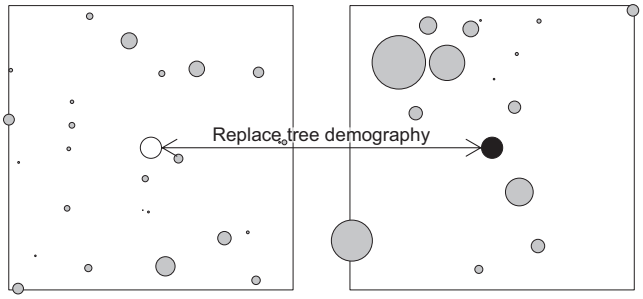

FIGURE 2 Generation of identity-free data from measurements by replacing tree demography between each pair of trees with the most similar stem diameters. The two squares represent two distinct local sites from within the entire plot, where each of the paired trees is at the centre. Circles show trees, and the size of circles indicates initial tree diameter. In the identity-free data, tree diameters in two censuses are replaced between the pair of trees (white vs. black circle). This replacement was performed for every other pair of trees so that all trees were swapped once

recruitment are independent of species identity and site (e.g. topography, soil, neighbours and shade).

We examined variation in turnovers for biomass B (Mg/ha) and in tree density or abundance N (ha^{-1}) for each species population as follows. We denoted the individual-tree above-ground oven-dry biomass (Mg) of a tree i in the first and second census by W_{0i} and W_{Ti} respectively. If a tree i was recorded in the first census but then died before the second, we set $W_{Ti} = 0$; else if a tree i recruited and was recorded only in the second census, $W_{0i} = 0$. We denoted the state of survival s_i, and that of death d_i, such that $s_i = 1$ only if a tree i was alive in both censuses (otherwise $s_i = 0$), and that $d_i = 1$ only if i died during censuses. The third state, that a tree i recruited, is thus $1 - s_i - d_i$. Above-ground biomass of a species population at the first and second census are $B_0 = \Sigma_i W_{0i}/A$ and $B_T = \Sigma_i W_{Ti}/A$ (Mg/ha) for all i's, respectively, and the first census biomass for trees that survived until second census is $Bs_0 = \Sigma_i s_i W_{0i}/A$, where A (ha) is the horizontal land area of plot (or subplot). Tree density, or abundance of species in the two censuses are $N_0 = \Sigma_i(s_i + d_i)/A$ and $N_T = \Sigma_i(1 - d_i)/A$(ha^{-1}), respectively, and that survived over two censuses is $Ns = \Sigma_i s_i/A$.

We estimated the instantaneous production and loss of biomass B of each species based on a 'continuous-time' model,

$$dB/dt = (p - l)\,B, \tag{1}$$

where p (year^{-1}) is relative (= per-biomass) production, or relative productivity, by tree growth including recruits' ingrowth, and l (year^{-1}) is relative loss by tree mortality (see Kohyama et al., 2019). For the dynamics of abundance N, we employed the same formulation as Equation 1:

$$dN/dt = (r - m)\,N, \tag{2}$$

where r and m are instantaneous per-capita recruitment and mortality, respectively (Kohyama, Kohyama, & Sheil, 2018). If the time interval between two censuses is identical at T (year) across all trees, we obtain turnover estimates as: $p = \ln(B_T/Bs_0)/T$, $l = \ln(B_0/Bs_0)/T$, $r = \ln(N_T/Ns)/T$ and $m = \ln(N_0/Ns)/T$ (Kohyama et al., 2018, 2019). However, because census duration varies among trees in the Pasoh plot data, we employed the following implicit equations of turnover obtained by time integration of Equations 1 and 2 from $t = 0$ to T_i for every tree i,

$$\sum_i W_{Ti}\exp(-pT_i) = \sum_i s_i W_{0i}, \tag{3}$$

$$\sum_i W_{0i}\exp(-lT_i) = \sum_i s_i W_{0i}, \tag{4}$$

$$\sum_i (1-d_i)\exp(-rT_i) = \sum_i s_i, \text{ and} \tag{5}$$

$$\sum_i (s_i+d_i)\exp(-mT_i) = \sum_i s_i. \tag{6}$$

We solved Equations 3–6 using the Newton–Raphson method (cf. Kohyama et al., 2018; Kubo, Kohyama, Potts, & Ashton, 2000). We note that these descriptive estimates of turnover are prone to estimation errors. Per-capita vital rate estimates (r, m) are influenced by the count of states, that is, survival, death and recruitment (Kohyama et al., 2018) and per-biomass rates (p, l) are influenced by those events as well as measurement errors of dbh. In the next section we introduce statistical models to quantify dbh-dependent growth and mortality of each species population by the combination of community-wide model parameters and species-specific deviation from those (as random effect). We compare (p, l) and these statistical estimates of growth and mortality at the largest population tree size.

We quantified period-mean population biomass B (and so for leaf biomass, denoted B_L) and tree density N during the period over two censuses (Kohyama et al., 2018, 2019) as

$$B = \left(B_T - B_0\right)/\ln\left(B_T/B_0\right), \text{ and} \tag{7}$$

$$N = \left(N_T - N_0\right)/\ln\left(N_T/N_0\right). \tag{8}$$

In addition to B and N, we quantified each species population by the 99 percentile tree biomass W_{max} (Mg) as a standardized maximum tree size to avoid the effect of population size N (Kohyama et al., 2015).

Plot-level biomass B_{plot} is $\Sigma_k B$, where k denotes species (including the aggregated population of all rarer species). Plot-level absolute

production by tree growth and recruitment, P_{plot} and absolute loss by tree death L_{plot} are:

$$P_{plot} = \sum_k pB, \text{ and } L_{plot} = \sum_k lB.$$

(Kohyama et al., 2019).

Niiyama, Ripin, Yasuda, Sato, and Shari (2019) compiled the records of monthly rate of fine litter fall, that is, leaves, reproductive organs, twigs and bark, etc., in 100 traps of 50 m^2 in total, over 25 years in the Pasoh forest. We employed the records of the 8 years from June 1992 to May 2000, the period overlapped with the examined two tree censuses. By denoting the absolute rate of fine litter fall F (Mg ha^{-1} $year^{-1}$), and assuming no loss between production and fall of these fine parts, we obtained an estimate of above-ground net primary production NPP to be:

$$\text{NPP} = P_{plot} + F.$$

2.2 | Stem-size dependence of individual growth and mortality

We used the plot-wide Bayesian procedure (Kohyama et al., 2015) to estimate tree-size-dependent growth for each tree of species. We fitted a curve relating relative rate of biomass increase of a surviving tree i of period-mean biomass $W = (W_{Ti} - W_{0i})/\ln(W_{Ti}/W_{0i})$ (cf. Equations 6 and 7), $g(W) = \ln(W_{Ti}/W_{0i})/T_i$ ($year^{-1}$), with respect to period-mean dbh D (cm) using,

$$g(W) = \alpha D^{\beta}\exp(\gamma D) = \alpha[f(W)]^{\beta}\exp[\gamma f(W)], \quad (9)$$

where $D = f(W)$ is the reverse function of the set of allometric functions by Niiyama et al. (2010). We determined a nearly perfect approximation $f(W) = 22.4W^{0.326}\exp(0.283W^{0.203})$. We approximated among-tree variation in $g(W)$ at any given W by exponential distribution, and accounted for dbh measurement error. Similarly, we fitted a curve relating tree mortality of a tree i at $W = W_{0i}$, $\mu(W) = \ln[(s_i + d_i)/s_i]/T_i$, using the formula as Equation 9, where the probability d_i/s_i followed Bernoulli distribution. We set all (α, β, γ)'s of $g(W)$ and $\mu(W)$ for each species to the plot-wide value and a species-specific parameter. Treatment of measurement error and model-parameter priors follows those in Kohyama et al. (2015).

2.3 | Other plot data

We performed similar analyses using data from four other old-growth mixed forests. Serimbu plots (two plots, 1 ha each and combined in the analysis) are located in an intact lowland mixed dipterocarp forest (0°45′N, 110°06′E) in West Kalimantan (Kohyama et al., 2003). We used censuses from 1992 and 1995 (3 years). We also analysed data from Ulu Gadut old-growth foothill dipterocarp forest in West Sumatra (Pinang Pinang plot of 1 ha at 0°55′S, 100°30′E). Here we used censuses from 1984 to 2004 (Kohyama et al., 2019). We also analysed data from old growth warm-temperate rain forest using 1998 and 2008 plot census data from the Segire and Koyohji basin (30°20′N, 130°50′E; 0.89 ha in total area) in Yakushima Island, southern Japan (Kohyama, 1993). Data for intact cool-temperate mixed deciduous forest (42°37′N, 141°36′E) was drawn from the 4-ha plot located in Tomakomai, Hokkaido (Kohyama et al., 2019). We used censuses in 1996 and 2006 (10 years). In all plots, we selected species with ≥6 trees surviving over the period with ≥5 cm dbh (but ≥8 cm for Ulu Gadut). We used plot-specific tree height versus dbh allometry, and biomass equations of Niiyama et al. (2010) for the two Indonesian rain forests, Ishihara et al. (2015) for warm-temperate rain forests on Yakushima, and the site-specific ones for Tomakomai (Kohyama et al., 2019).

2.4 | Statistical analysis

We fitted species-level relative productivity p (and other turnover rates, l, r and m) to population biomass B (and W_{max} and N), using an Equation 9 type model

$$p = aB^b\exp(cB), \quad (10)$$

which fits log-nonlinear p–B relationship with parameters (a, b, c). We tested whether the reduced log–log linear, power function model, $p = aB^b$, was a better model than the full model of Equation 10. For subplot-nested model, we described local (= per-subplot) species-level relative productivity, p ($year^{-1}$), as a function of local species biomass B (Mg/ha) and species-sum subplot-level biomass $B_{subplot}$ (Mg/ha),

$$p = aB^b\exp(cB)B_{subplot}{}^d. \quad (11)$$

with four parameters (a, b, c, d) to be estimated. To relate population-level leaf mass B_L (Mg/ha) to species above-ground biomass B (cf. our Hypothesis 4), Equation 10 or simpler power function is not applicable because B_L should be smaller than B. We therefore used the following allocation equation

$$B_L = a'c'B/\left(a' + c'B^{-b'}\right), \quad (12)$$

where (a', b', c') are parameters (a' and c' are positive). Leaf mass ratio B_L/B is c' for B to be close to zero, and is approximately a power function $a'B^{b'}$ for infinite B. We ran linear and nonliner regressions on log-transformed Equations 10–12, based on the examination of residual distributions (Xiao, White, Hooten, & Durham, 2011), and applied model selection by AIC. We used R 3.4.1 (R Core Team, 2017) for all calculation and analysis, and JAGS 4.3.0 (Pullmer, 2017) for the MCMC simulation of estimating Equation 9 parameters, of which R code is in the Dryad repository for Kohyama et al. (2015): https://doi.org/10.5061/dryad.bb460. The Pasoh datasets of 1990 and 2000 plot inventories for observed and identity-free community, and R code to obtain species-specific structural data (B, B_L, W_{max}, N) and turnover rates (p, l, r, m) from these datasets are provided in the GitHub/Zenodo repository for this paper: https://github.com/kohyamat/p-B (https://doi.org/10.5281/zenodo.3966750).

3 | RESULTS

3.1 | Interspecific variation in turnover

There were 390 species with 100 or more surviving individuals, $\Sigma_i s_i \geq 100$ (out of 808 recorded species in total). These 390 species comprised 94.7% of the total tree density (N_{plot} = 6,155.6/ha), and 90.3% of total biomass (B_{plot} = 467.8 Mg/ha) in the Pasoh 50-ha plot. The three species with the highest biomass were all dipterocarps that could reach the canopy: *Neobalanocarpus heimii* (B = 21.9 Mg/ha), *Shorea leprosula* (21.7 Mg/ha) and *S. maxwelliana* (19.8 Mg/ha). The species with the least biomass were small-stature shrubs—*Tetrardisia porosa* (0.000886 Mg/ha) and *Semecarpus curtisii* (0.00152 Mg/ha). Therefore, biomass per species spanned four orders of magnitude. Plot-scale species biomass B was relatively well predicted by powers of standardized maximum tree mass W_{max} and tree density N as $B = 0.0781 W_{max}^{0.824} N^{0.912}$ (R^2 = 0.971, W_{max} ΔR^2 = 0.902 and N ΔR^2 = 0.202).

Observed species turnover varied 10-fold or more among the 390 species. Relative production p ranged from 0.0098 to 0.0638/year (95% range) and the median was 0.0262/year. Turnover in species biomass (p, l) and stem density (r, m) were all positively correlated; correlation coefficients (R's) were ranging from 0.300 to 0.570 (Table S1). Thus, species with high-biomass turnover showed high stem turnover. In contrast, in the identity-free data (where we recorded 395 'species' ≥100 survived trees), most of these correlations were markedly lower. Their correlation coefficients ranged from 0.069 to 0.375 (Table S1).

The relative production p and species biomass B appear inversely related among the 390 species. The power function model, $p = aB^b$, was selected by fitting Equation 10, that is, $c = 0$ (Figures 3a and 4a). The power exponent b for p on B in observed community was −0.128 (with 95% confidence interval, henceforth 'CI', of −0.150 and −0.105, Figure 4a). The aggregated population of the rarer 418 species (accounting for 5.3% of plot total biomass) showed a relative productivity of p = 0.0232/year, which is located above the regression line for the other, more abundant, 390 species (Figure 3a). In the identity-free community, p–B exponent was −0.218 with CI [−0.239, −0.197], which was significantly more negative than that in the observed community (Figures 3b and 4a). For the observed data, relative biomass loss l decreased with B (Figure 3c), and the exponent −0.106 was not significantly different from the p–B exponent at −0.128 (Figure 4a). Therefore, the net rate of biomass change, p–l (year^{-1}), indicated by coloured dots in Figure 3, showed no clear dependence on species biomass (Figure 3a,c). The sum of rare species showed a higher biomass loss rate than did the highest biomass

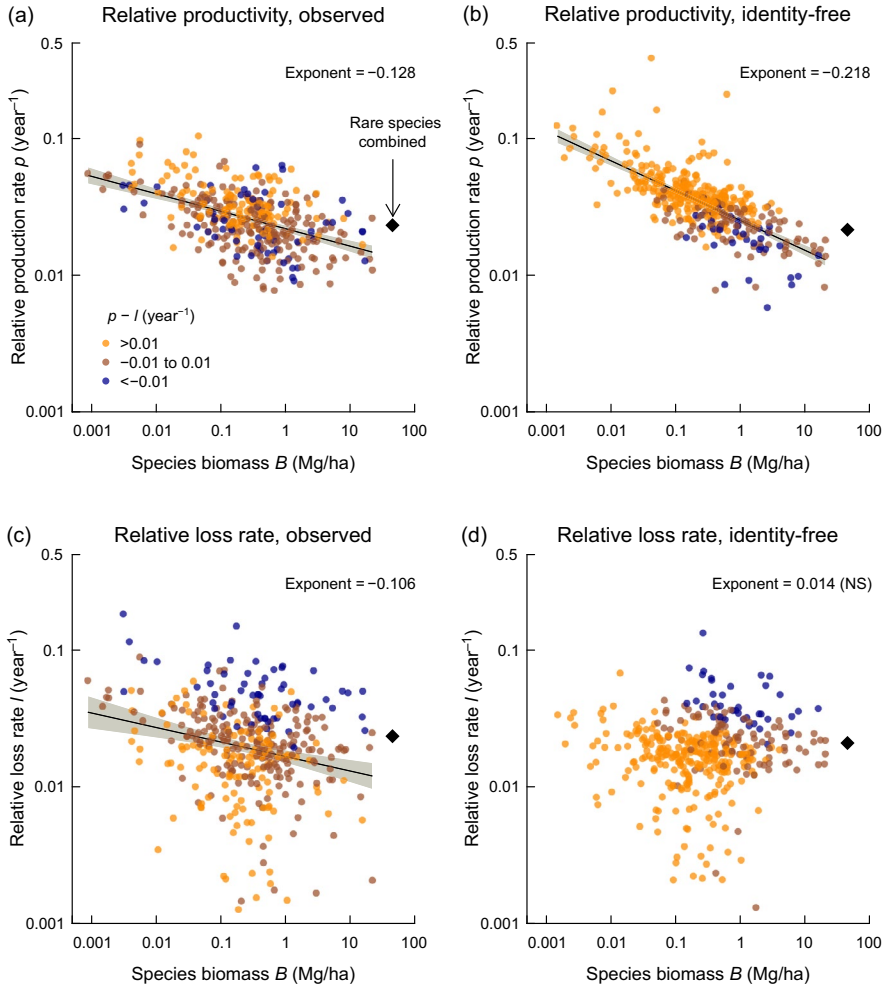

FIGURE 3 Interspecific relationship of per species biomass turnover to biomass in the Pasoh data. (a) Relative production p among observed 390 species; (b) relative production among 395 identity-free species; (c) relative loss l among observed species; and (d) relative loss among identity-free species. Dot colours correspond to decreasing (blue) to increasing (orange) biomass in net change rate, $p - l$. Regression using a power function with 95% confidence interval is shown, and estimated exponent, or log–log slope, is stated in each panel. The black square indicates the aggregated data for the combined rare species

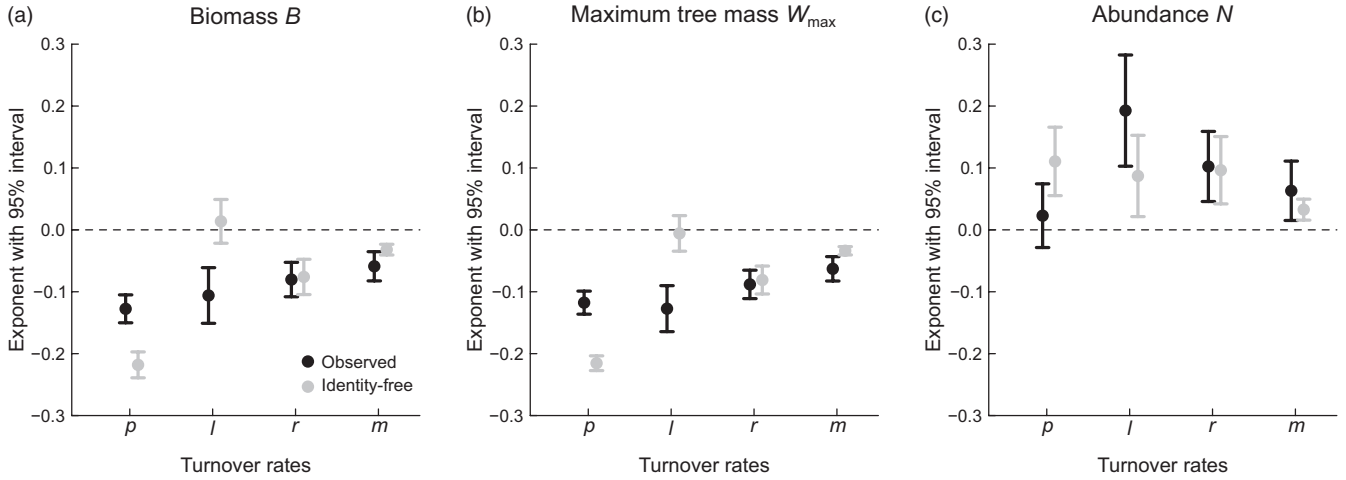

FIGURE 4 Estimated power exponent and 95% confidence interval for interspecific relationships of turnover on species structure metrics in the Pasoh data. Turnover are relative (= per-unit biomass) productivity *p* and loss *l*, per-capita recruitment *r* and mortality *m* (all in year^{-1}); species structure metrics are (a) biomass *B* (Mg/ha), (b) 99% tree mass W_{max} (Mg), (c) abundance *N* (ha^{-1}). Black and grey for observed and identity-free data respectively

FIGURE 5 Population-level leaf mass ratio LMR and per-leaf-mass productivity *p*/LMR, plotted against species biomass in the Pasoh data. (a) LMR among observed species, and (b) among identity-free species. Regression curves with 95% confidence interval were estimated using Equation 12. (c) Per-leaf-mass production rate, *p*/LMR, among observed species, and (d) among identity-free species, fitted by power function with 95% confidence interval; exponent is shown. Dot colours indicate net rate of biomass change, $p - l$

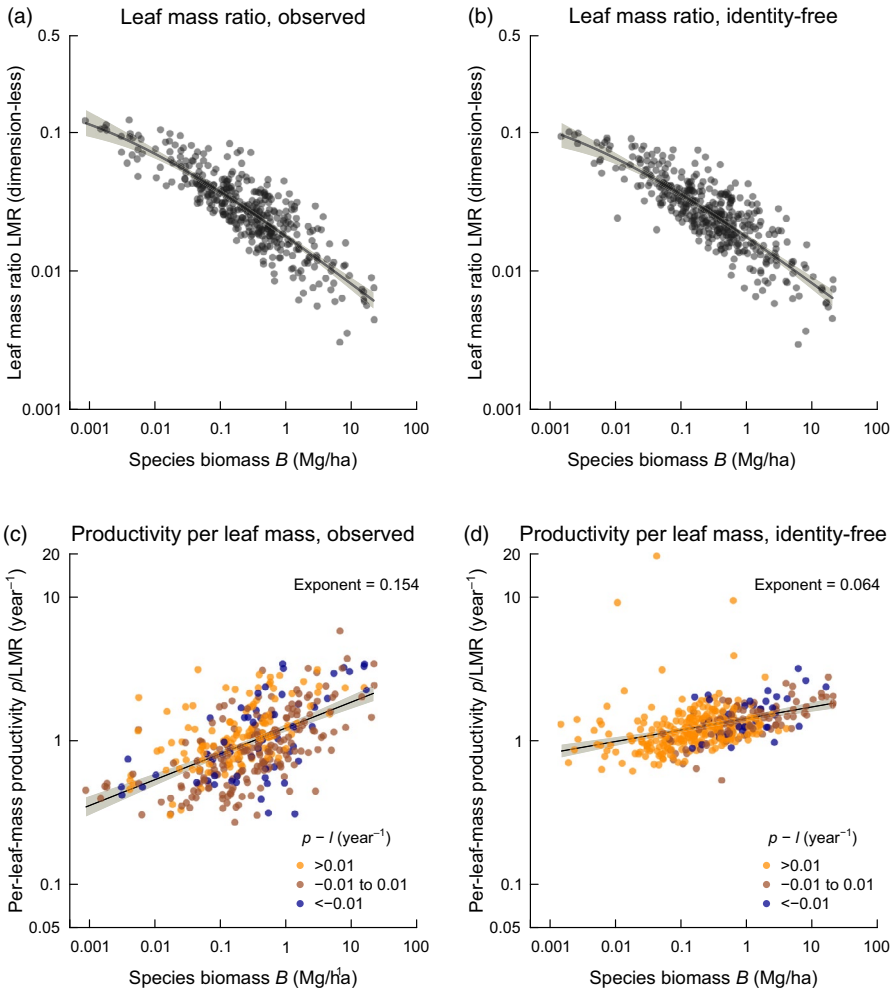

species (Figure 3c). In contrast for the identity-free data, the *l*–*B* exponent was not different from zero (Figure 3d) and thus was distinct from the *p*–*B* exponent (Figure 4a). As a result, the *B* values of the identity-free 'species' with smaller *B* tended to increase ($p - l > 0$), while the values for those 'species' with larger *B* were more likely to decline (Figure 3b,d).

Per-capita recruitment *r* and mortality *m* also decreased with species biomass *B* in observed data (Figure 4a). The power exponent of *r* on

B was not significantly different from that of *p* on *B*, but the *m*–*B* exponent of −0.059 was larger than the *p*–*B* exponent of −0.128 (Figure 4a).

Because species biomass *B* was strongly correlated with maximum tree mass W_{max}, turnover (*p*, *l*, *r*, *m*) decreased with W_{max} (Figure 4b), and was similar to turnover dependence on *B* (Figure 4a). In contrast to the clear link between turnover with *B* and W_{max}, we found no significant correlation between *p* and tree density *N*, and increasing *l*, *r* and *m* with *N* in the observed data (Figure 4c).

Among the 390 species, 21 species are considered 'pioneers' (Davies et al., 2003). These species generally had larger *p* for small biomass species, and a steeper decline of *p* on *B*; the *p*–*B* exponent for pioneers was −0.34 with CI [−0.54, −0.16] (Figure S1a). We observed no clear variation in the *p*–*B* relationship due to interspecific differences in stem wood density when we consider the 210 tree species that appear in the Global Wood Density Database (Zanne et al., 2009; Figure S1b).

3.2 | Linkage with population-level leaf mass ratio

Among species, population-level leaf mass ratio, LMR = B_L/B, exhibited a negative correlation with above-ground biomass *B* in both the observed and identity-free community, which was approximated using Equation 12 (Figure 5a,b). Per-leaf-mass productivity, $p/\text{LMR} = P/B_L$ (year^{-1}) increased with species biomass in observed and identity-free forests (Figure 5c,d) though the slope was significantly less for the latter.

3.3 | Linkage with individual tree growth and mortality

Tree relative growth rate, $g(W)$, decreased with tree mass *W* (Figure 6a). Species with large standardized maximum mass W_{max} tended to grow faster than species with small W_{max} at the same reference sizes up to 36 cm dbh (at 5% significance level). By contrast, relative growth at maximum size, $g(W_{max})$, was significantly negatively correlated with W_{max} among species (Figure 6a), because $g(W)$ sharply decreased around W_{max} for most species. Individual tree mortality $\mu(W)$ was typically lower at intermediate tree sizes for most species (Figure 6b). Tree-size-dependent mortality $\mu(W)$ was negatively correlated with species W_{max} over reference tree sizes up to 64 cm dbh, and so was $\mu(W_{max})$ with W_{max} (Figure 6b, significant at 5%). Population-level relative productivity *p* was closely positively correlated to individual tree relative growth at W_{max}, $g(W_{max})$ (Figure 6c, $R^2 = 0.813$ in log–log linear regression). Similarly, the population-level relative loss *l* was positively correlated with tree mortality at W_{max}, $\mu(W_{max})$ (Figure 6d, $R^2 = 0.592$).

3.4 | Productivity dependence on subplot-by-species structure

To evaluate spatial variation in the interspecific productivity–biomass relationship, we calculated the biomass and relative production of local species populations in two hundred 0.25-ha subplots. Selected

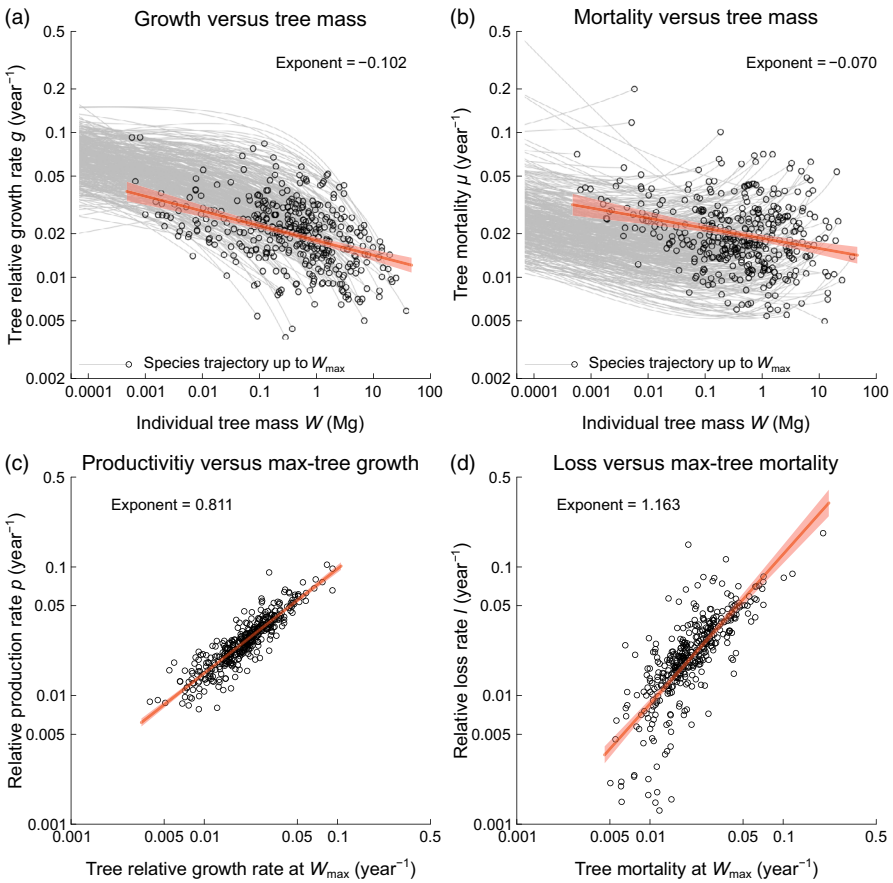

FIGURE 6 Interspecific variation in tree-level relative growth and mortality among observed 390 species in the Pasoh plot data. (a) Relative growth $g(W)$ versus tree mass *W*; and (b) tree mortality $\mu(W)$ versus tree mass, fitted by Equation 9. Among-species regression of $g(W_{max})$ and $\mu(W_{max})$ on W_{max} (by open circles) are indicated by coloured lines with 95% confidence interval. (c) Plot of species-level relative production *p* versus maximum tree mass relative growth, $g(W_{max})$; (d) Plot of species-level relative biomass loss *l* versus maximum tree size mortality, $\mu(W_{max})$. Coloured lines in (c) and (d) show power function fits (with 95% confidence interval, see inset for exponent values)

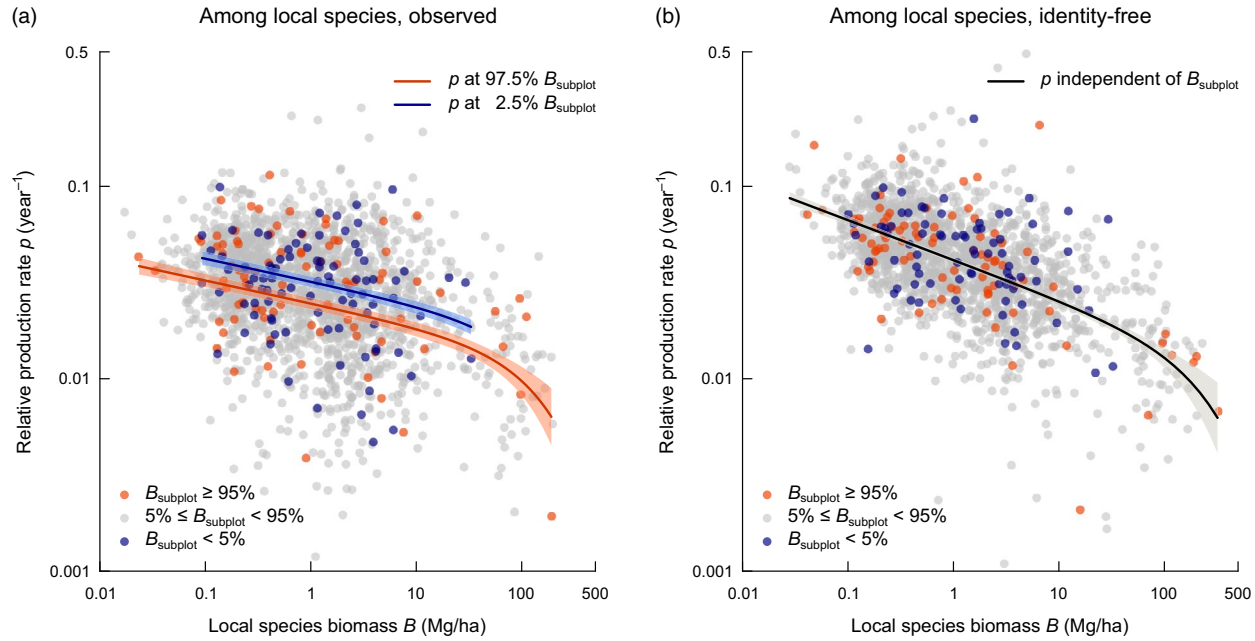

FIGURE 7 Relationship of estimated relative production versus biomass of local species populations in the Pasoh plot data. *B*, local species biomass; $B_{subplot}$, species-sum subplot biomass in 0.25 ha. Fitted curve (with 95% confidence interval) using Equation 11 shown. (a) Plot of observed species populations with two curves at high and low $B_{subplot}$; (b) Plot of identity-free species populations with the curve independent of $B_{subplot}$ effect. Local species populations with non-positive *p* (16 out of 2,036 local populations in observed, 6 out of 1,951 in identity-free) are excluded in model fitting

abundant species at each subplot had ≥20 surviving trees. The observed local species populations at this quarter hectare scale showed a broader scatter when *p* was plotted against local species biomass *B* (Figure 7a) than for the full 50 ha (Figure 3a). Among these populations, *p* on local species biomass *B* exhibited an upward convex curve on a log–log scale, and observed *p* on *B* relationships for these subplots with stand-level biomass $B_{subplot}$ supported the full model of Equation 11 with model parameters *b*, *c* and *d* all being negative (Figure 7a). In contrast, identity-free local 'species' populations showed less variation in *p* on *B* relationship and supported a reduced model of Equation 11 without $B_{subplot}$ dependence, that is, parameter $d = 0$ (Figure 7b).

3.5 | Plot-level net primary productivity

Estimated species-sum absolute productivity for the Pasoh plot P_{plot} was 10.0 Mg ha^{-1} year^{-1}, with a period-mean plot biomass B_{plot} of 468 Mg/ha. The rate of fine litter fall *F* was 6.49 ± 1.35 Mg ha^{-1} year^{-1} (of which leaf litter was 69%). The estimated plot-scale net primary production (NPP) was 16.5 Mg ha^{-1} year^{-1}, of which fine litter comprised 39%. Table S2 summarizes the different values estimated using conventional approaches that ignore interspecific variation.

3.6 | Interspecific productivity variation in other forests

Analysis of repeated census data from four other old-growth forests showed that relative productivity *p* declined with species biomass *B* (Figure S2). Despite the difference in plot biomass and productivity among forests, the distribution of species on the (*p*, *B*) coordinates did not show clear separation between those forests.

4 | DISCUSSION

We examined how constituent tree species populations with varied structural properties and demographic characteristics contribute to stand-level properties of net primary productivity in species-rich forests. We found that for the 390 most abundant species in the Pasoh 50-ha plot, species with larger population-level biomass also tended to be those with larger maximum individual tree biomass (cf. Hypothesis 1). Species-level relative production *p* was lower when species above-ground biomass *B* was higher and vice versa (cf. Hypothesis 2, Figure 3a). We also found that the sum of rarer species (<100 stems per plot) showed higher productivity compared to high-biomass species (Figure 3a). The proportion of leaf mass in above-ground biomass was lower among populations with higher species overall biomass (cf. Hypothesis 3, Figure 5a). A negative *p*–*B* relationship reflects that larger stemmed species typically possess lower relative growth at their largest stem sizes than smaller stemmed species (cf. Hypothesis 4; Figure 6a). Comparable relationships were observed in four other old-growth forests suggesting similar processes.

The variation in per-species turnover in biomass (relative productivity and loss) and abundance (per-capita recruitment and mortality) was positively correlated in the Pasoh Forest. Species turnover in biomass and abundance were negatively related to species biomass *B* and maximum tree mass W_{max} (Figure 4a,b), suggesting that

interspecific variation in *B* is maintained over time. In contrast, in the identity-free community, the relationship between *p*–*B* was negative while *I*–*B* was neutral (Figures 3b,d and 4a), thus 'species' biomass changes with time. Our results appear consistent with patterns reported in other old-growth tropical forests. For example, Nascimento et al. (2005) noted that abundance turnover rates (recruitment and mortality) were negatively correlated with mean tree size among 95 Amazonian tree species.

In some respects, the patterns we found among co-occurring tree populations in species-rich forests resemble those seen among dominant life forms across various biomes, where populations of organisms that reach larger dimensions have slower turnover than those with smaller body size (Brown, Gillooly, Allen, Savage, & West, 2004; Niklas & Enquist, 2001; Price, Gillooly, Allen, Weitz, & Niklas, 2010). Within-community trade-off between turnover and adult stature would partly reflect general life-history constraints shown by these studies. In addition, within-community interspecific productivity partitioning is also regulated by interactions among individual-stems in the shared habitat. For example, we found small-stature species with low *B* show lower productivity per unit leaf mass than large-stature species (Figure 5c). This is presumably because small species typically have less access to light on average. Our examination of the variation in production among subplot-scale species populations suggests that species productivity *p* in a local subplot is negatively correlated to both local species-level biomass and species-sum subplot-level biomass (Figure 7a), but not in identity-free forest where variation in demography is (we presume) independent of local stand conditions (Figure 7b). Higher *p* at the same species biomass in less-crowded local stands indicates that the productivity of species populations is regulated by local-scale available resources, such as light.

Our study clarifies why large species tend to show low relative productivity regardless of the well-established fact that trees of larger stature species tend to grow faster than those of smaller stature species over a range of reference stem diameters (Iida et al., 2014; King, Davies, et al., 2006; King, Wright, et al., 2006; Kohyama et al., 2003, 2015; Lieberman et al., 1985; Poorter et al., 2008; Rüger et al., 2018). The higher growth observed for larger stature species likely reflects that their juveniles tend to appear in less shaded conditions than stems of smaller stature species (Sheil, Salim, Chave, Vanclay, & Hawthorne, 2006), and that shorter species favour higher reproductive allocation rather than vegetative growth at the same stem sizes (King, Wright, et al., 2006; Kohyama et al., 2003). By comparing species at W_{max}, we obtained contrasting patterns of interspecific variation. Because of the generally marked reduction of relative growth observed at large stem sizes, larger sized species also experienced lower $g(W_{max})$ than smaller sized species (Figure 6a). In contrast, stem mortality of larger sized species was low at the same stem sizes, and their $\mu(W_{max})$ compared to smaller sized species was generally lower, even though mortality tended to increase when species approached their largest stem sizes (Figure 6b). Fast growth and generally low mortality (at most sizes) for juveniles of large-stature species result in a low mortality-to-growth ratio, which allows a species population to reach larger maximum sizes (Kohyama et al., 2015). However, close to their maximum size, larger sized species show slower relative growth and survive longer than smaller sized species, resulting in similar negative power exponents between *p*–*B* and *I*–*B* relationship in the observed (but not in the identity-free) community (Figures 3 and 6).

The variation in demographic characteristics among coexisting tree species has been related to horizontal and vertical aspects of forest structure. Variation in understorey light enhances interspecific differentiation in juvenile growth, survival and shade-tolerance sometimes called 'the growth-survival trade-off' (Rees, Condit, Crawley, Pacala, & Tilman, 2001; Wright et al., 2010; Zhu et al., 2018). In contrast, in terms of the vertical structure of the forest canopy, we observe interspecific differentiation between short stature species exhibiting high reproductive allocation for frequent recruitment and tall stature species showing high allocation to vegetative growth for height gain (and delayed reproduction), which is called 'the recruitment versus stature trade-off' (Falster et al., 2017; Kohyama, 1993; Kohyama & Takada, 2009; Rüger et al., 2018). Our results indicate that this trade-off between turnover and adult stature underlies the relationship between relative productivity and standing biomass. To generalize, we see that large-stature, high-biomass species show slower turnover—that is lower recruitment, relative growth and mortality—than small-stature species. We note that the greater range of species sizes that can occur in taller forests, and the associated diversity of size-dependent species behaviours this permits, explains why taller forests tend to be both more productive, and richer in species, than otherwise comparable forests of smaller stature (Duivenvoorden, 1996; Huston, 1994; Sheil & Bongers, 2020).

Improved methods that avoid major biases offer new insights that were not previously available. For example, we can now recognize the contribution that small-stature tree species make to both diversity and stand dynamics. High tree species diversity in tropical forests is known to be largely related to the diversity and persistence of small-sized species (King, Wright, et al., 2006; Niklas, Midgley, & Rand, 2003). We observed that the abundance of small-sized species with high relative productivity collectively contributes to high tropical forest net primary productivity—a contribution which was previously unnoticed due to the biases in previous 'conventional' production estimates (Kohyama et al., 2019).

Viewed in their totality, our results show how demographic differences among species contribute to general properties of ecosystem functioning and biodiversity maintenance. Small-stature, low-biomass species contribute to high forest net primary productivity and enhance ecosystem resilience through rapid biomass turnover and replacement via high per-capita recruitment and relative productivity. In contrast, large-stature species contribute to the persistence of large biomass storage by their longevity (low mortality). The mass ratio hypothesis posits that species-level biomass in a plant community is proportional to species' absolute (not relative) rates of primary production and nutrient supply to soil heterotroph,

and thus high-biomass species disproportionately control ecosystem functioning (Grime, 1998). Studies that consider the role of functional diversity have suggested that ecosystem properties predominantly reflect the characteristics of higher biomass species (Finegan et al., 2015; Fotis et al., 2018; Prado-Junior et al., 2016). In contrast, our study implies that the contribution of biodiversity to ecosystem functioning is more complex and multidimensional with different populations making distinct and disproportionate contributions to different ecosystem properties. For example, ecosystem resilience and biomass recovery depend disproportionately on species with rapid turnover while standing biomass and total carbon sequestration depend disproportionately on species with slow turnover.

ACKNOWLEDGEMENTS

We acknowledge that the project of Pasoh 50-ha Forest Dynamics Plot is carried out by the Forest Research Institute Malaysia and Center for Tropical Forest Science–Forest Global Earth Observatory. We thank David Gibson, Gerhard Zotz and two reviewers for valuable suggestions. This study was supported by Grant-in-Aid for Scientific Research from the Japan Society for the Promotion of Science (18H02504). Authors declare no competing financial interests or other conflicts of interest.

AUTHORS' CONTRIBUTIONS

T.S.K., D.S. and M.D.P. designed the project; T.L.Y. and S.J.D. updated plot data; K.N. compiled biomass data; T.S.K. and T.I.K. carried out numerical analysis; T.S.K. drafted; D.S., S.J.D. and M.D.P. revised the conceptual framing and all authors approved the paper for publication.

PEER REVIEW

The peer review history for this article is available at https://publons.com/publon/10.1111/1365-2745.13485.

DATA AVAILABILITY STATEMENT

Observed and identity-free dataset of the Pasoh plot, and source code for estimation of population structural variables and turnover variables are provided in the GitHub repository and has been archived on Zenodo https://github.com/kohyamat/p-B; https://doi.org/10.5281/zenodo.3966750 (Kohyama et al., 2020).

ORCID

Takashi S. Kohyama https://orcid.org/0000-0001-7186-8585
Tetsuo I. Kohyama https://orcid.org/0000-0002-4567-2893
Douglas Sheil https://orcid.org/0000-0002-1166-6591

REFERENCES

Bastin, J.-F., Rutishauser, E., Kellner, J. R., Saatchi, S., Pélissier, R., Hérault, B., … Zebaze, D. (2018). Pan-tropical prediction of forest structure from the largest trees. *Global Ecology and Biogeography*, *27*(11), 1366–1383. https://doi.org/10.1111/geb.12803

Brown, J. H., Gillooly, J. F., Allen, A. P., Savage, V. M., & West, G. B. (2004). Toward a metabolic theory of ecology. *Ecology*, *85*(7), 1771–1789. https://doi.org/10.1890/03-9000

Chisholm, R. A., Muller-Landau, H. C., Abdul Rahman, K., Bebber, D. P., Bin, Y., Bohlman, S. A., … Zimmerman, J. K. (2013). Scale-dependent relationships between tree species richness and ecosystem function in forests. *Journal of Ecology*, *101*(5), 1214–1224. https://doi.org/10.1111/1365-2745.12132

Clark, D. A., Brown, S., Kicklighter, D. W., Chambers, J. Q., Thomlinson, J. R., Ni, J., & Holland, E. A. (2001). Net primary production in tropical forests: An evaluation and synthesis of existing field data. *Ecological Applications*, *11*(2), 371–384. https://doi.org/10.1890/1051-0761(2001)011[0371:NPPITF]2.0.CO;2

Condit, R., Ashton, P. S., Manokaran, N., LaFrankie, J. V., Hubbell, S. P., & Foster, R. B. (1999). Dynamics of the forest communities at Pasoh and Barro Colorado: Comparing two 50-ha plots. *Philosophical Transactions of the Royal Society of London B: Biological Sciences*, *354*(1391), 1739–1748.

Condit, R., Sukumar, R., Hubbell, S. P., & Foster, R. B. (1998). Predicting population trends from size distributions: A direct test in a tropical tree community. *The American Naturalist*, *152*(4), 495–509. https://doi.org/10.1086/286186

Coomes, D. A., & Allen, R. B. (2007). Mortality and tree-size distributions in natural mixed-age forests. *Journal of Ecology*, *95*(1), 27–40. https://doi.org/10.1111/j.1365-2745.2006.01179.x

Davies, S. J., Noor, N. S. M., LaFrankie, J. V., & Ashton, P. S. (2003). The trees of Pasoh Forest: Stand structure and floristic composition of the 50-ha forest research plot. In T. Okuda, N. Manokaran, Y. Matsumoto, K. Niiyama, S. C. Thomas, & P. S. Ashton (Eds.), *Pasoh: Ecology of a lowland rain forest in Southeast Asia* (pp. 35–50). Tokyo, Japan: Springer.

Duivenvoorden, J. F. (1996). Patterns of tree species richness in rain forests of the middle Caqueta area, Colombia, NW Amazonia. *Biotropica*, *28*(2), 142–158. https://doi.org/10.2307/2389070

Enquist, B. J., & Niklas, K. J. (2002). Global allocation rules for patterns of biomass partitioning in seed plants. *Science*, *295*(5559), 1517–1520. https://doi.org/10.1126/science.1066360

Falster, D. S., Brännström, Å., Westoby, M., & Dieckmann, U. (2017). Multitrait successional forest dynamics enable diverse competitive coexistence. *Proceedings of the National Academy of Sciences of the United States of America*, *114*(13), E2719–E2728. https://doi.org/10.1073/pnas.1610206114

Finegan, B., Peña-Claros, M., de Oliveira, A., Ascarrunz, N., Bret-Harte, M. S., Carreño-Rocabado, G., … Poorter, L. (2015). Does functional trait diversity predict above-ground biomass and productivity of tropical forests? Testing three alternative hypotheses. *Journal of Ecology*, *103*(1), 191–201. https://doi.org/10.1111/1365-2745.12346

Fotis, A. T., Murphy, S. J., Ricart, R. D., Krishnadas, M., Whitacre, J., Wenzel, J. W., … Comita, L. S. (2018). Above-ground biomass is driven by mass-ratio effects and stand structural attributes in a temperate deciduous forest. *Journal of Ecology*, *106*(2), 561–570. https://doi.org/10.1111/1365-2745.12847

Grime, J. P. (1998). Benefits of plant diversity to ecosystems: Immediate, filter and founder effects. *Journal of Ecology*, *86*(6), 902–910. https://doi.org/10.1046/j.1365-2745.1998.00306.x

Hooper, D. U., Chapin, F. S., Ewel, J. J., Hector, A., Inchausti, P., Lavorel, S., … Wardle, D. A. (2005). Effects of biodiversity on ecosystem functioning: A consensus of current knowledge. *Ecological Monographs*, *75*(1), 3–35. https://doi.org/10.1890/04-0922

Huston, M. A. (1994). *Biological diversity: The coexistence of species*. Cambridge, UK: Cambridge University Press.

Iida, Y., Kohyama, T. S., Kubo, T., Kassim, A. R., Poorter, L., Sterck, F., & Potts, M. D. (2011). Tree architecture and life-history strategies across 200 co-occurring tropical tree species. *Functional Ecology*, *25*(6), 1260–1268. https://doi.org/10.1111/j.1365-2435.2011.01884.x

Iida, Y., Poorter, L., Sterck, F., Kassim, A. R., Potts, M. D., Kubo, T., & Kohyama, T. S. (2014). Linking size-dependent growth and mortality

with architectural traits across 145 co-occurring tropical tree species. *Ecology*, *95*(2), 353–363. https://doi.org/10.1890/11-2173.1

Ishihara, M. I., Utsugi, H., Tanouchi, H., Aiba, M., Kurokawa, H., Onoda, Y., … Hiura, T. (2015). Efficacy of generic allometric equations for estimating biomass: A test in Japanese natural forests. *Ecological Applications*, *25*(5), 1433–1446. https://doi.org/10.1890/14-0175.1

Jucker, T., Sanchez, A. C., Lindsell, J. A., Allen, H. D., Amable, G. S., & Coomes, D. A. (2016). Drivers of aboveground wood production in a lowland tropical forest of West Africa: Teasing apart the roles of tree density, tree diversity, soil phosphorus, and historical logging. *Ecology and Evolution*, *6*(12), 4004–4017. https://doi.org/10.1002/ece3.2175

King, D. A., Davies, S. J., & Noor, N. S. M. (2006). Growth and mortality are related to adult tree size in a Malaysian mixed dipterocarp forest. *Forest Ecology and Management*, *223*(1–3), 152–158. https://doi.org/10.1016/j.foreco.2005.10.066

King, D. A., Wright, S. J., & Connell, J. H. (2006). The contribution of interspecific variation in maximum tree height to tropical and temperate diversity. *Journal of Tropical Ecology*, *22*(1), 11–24. https://doi.org/10.1017/S0266467405002774

Kira, T., & Shidei, T. (1967). Primary production and turnover of organic matter in different forest ecosystems of the western Pacific. *Japanese Journal of Ecology*, *17*(2), 70–87.

Kohyama, T. (1993). Size-structured tree populations in gap-dynamic forest–the forest architecture hypothesis for the stable coexistence of species. *Journal of Ecology*, *81*(1), 131–143. https://doi.org/10.2307/2261230

Kohyama, T. S., Kohyama, T. I., & Sheil, D. (2018). Definition and estimation of vital rates from repeated censuses: Choices, comparisons and bias corrections focusing on trees. *Methods in Ecology and Evolution*, *9*(4), 809–821. https://doi.org/10.1111/2041-210X.12929

Kohyama, T. S., Kohyama, T. I., & Sheil, D. (2019). Estimating net biomass production and loss from repeated measurements of trees in forests and woodlands: Formulae, biases and recommendations. *Forest Ecology and Management*, *433*, 729–740. https://doi.org/10.1016/j.foreco.2018.11.010

Kohyama, T. S., Potts, M. D., Kohyama, T. I., Abd Rahman, K., & Ashton, P. S. (2015). Demographic properties shape tree size distribution in a Malaysan rain forest. *The American Naturalist*, *185*(3), 367–379.

Kohyama, T. S., Potts, M. D., Kohyama, T. I., Niiyama, K., Yao, T. L., Davies, S. J., & Sheil, D. (2020). Data from: Trade-off between standing biomass and productivity in species-rich tropical forest: Evidence, explanations and implications (Version v1.0.0) [Data set]. *Zenodo*, https://doi.org/10.5281/zenodo.3966750

Kohyama, T., Suzuki, E., Partomihardjo, T., Yamada, T., & Kubo, T. (2003). Tree species differentiation in growth, recruitment and allometry in relation to maximum height in a Bornean mixed dipterocarp forest. *Journal of Ecology*, *91*(5), 797–806. https://doi.org/10.1046/j.1365-2745.2003.00810.x

Kohyama, T., & Takada, T. (2009). The stratification theory for plant coexistence promoted by one-sided competition. *Journal of Ecology*, *97*(3), 463–471. https://doi.org/10.1111/j.1365-2745.2009.01490.x

Kubo, T., Kohyama, T., Potts, M. D., & Ashton, P. S. (2000). Mortality rate estimation when inter-census intervals vary. *Journal of Tropical Ecology*, *16*(5), 753–756. https://doi.org/10.1017/S026646740000170X

Liang, J., Zhou, M., Tobin, P. C., McGuire, A. D., & Reich, P. B. (2015). Biodiversity influences plant productivity through niche-efficiency. *Proceedings of the National Academy of Sciences of the United States of America*, *112*(18), 5738–5743. https://doi.org/10.1073/pnas.1409853112

Lieberman, D., Lieberman, M., Hartshorn, G., & Peralta, R. (1985). Growth rates and age–size relationships of tropical wet forest trees in Costa Rica. *Journal of Tropical Ecology*, *1*(2), 97–109. https://doi.org/10.1017/S026646740000016X

Ligot, G., Gourlet-Fleury, S., Ouédraogo, D.-Y., Morin, X., Bauwens, S., Baya, F., … Fayolle, A. (2018). The limited contribution of large trees to annual biomass production in an old-growth tropical forest. *Ecological Applications*, *28*(5), 1273–1281. https://doi.org/10.1002/eap.1726

Lutz, J. A., Furniss, T. J., Johnson, D. J., Davies, S. J., Allen, D., Alonso, A., … Zimmerman, J. K. (2018). Global importance of large-diameter trees. *Global Ecology and Biogeography*, *27*(7), 849–864. https://doi.org/10.1111/geb.12747

Malhi, Y., Baker, T. R., Phillips, O. L., Almeida, S., Alvarez, E., Arroyo, L., … Lloyd, J. (2004). The above-ground coarse wood productivity of 104 Neotropical forest plots. *Global Change Biology*, *10*(5), 563–591. https://doi.org/10.1111/j.1529-8817.2003.00778.x

Manokaran, N., & Kochummen, K. M. (1987). Recruitment, growth and mortality of tree species in a lowland dipterocarp forest in Peninsular Malaysia. *Journal of Tropical Ecology*, *3*(4), 315–330. https://doi.org/10.1017/S0266467400002303

Manokaran, N., & LaFrankie Jr, J. V. (1990). Stand structure of Pasoh Forest Reserve, a lowland rain forest in Peninsular Malaysia. *Journal of Tropical Forest Science*, *3*, 14–24.

Mori, A. S. (2018). Environmental controls on the causes and functional consequences of tree species diversity. *Journal of Ecology*, *106*(1), 113–125. https://doi.org/10.1111/1365-2745.12851

Nascimento, H. E., Laurance, W. F., Condit, R., Laurance, S. G., D'Angelo, S., & Andrade, A. C. (2005). Demographic and life-history correlates for Amazonian trees. *Journal of Vegetation Science*, *16*(6), 625–634. https://doi.org/10.1111/j.1654-1103.2005.tb02405.x

Niiyama, K., Kajimoto, T., Matsuura, Y., Yamashita, T., Matsuo, N., Yashiro, Y., … Noor, N. S. (2010). Estimation of root biomass based on excavation of individual root systems in a primary dipterocarp forest in Pasoh Forest Reserve, Peninsular Malaysia. *Journal of Tropical Ecology*, *26*(3), 271–284. https://doi.org/10.1017/S0266467410000040

Niiyama, K., Ripin, A., Yasuda, M., Sato, T., & Shari, N. H. Z. (2019). Data paper: Long-term litter production in a lowland dipterocarp forest, Peninsular Malaysia from 1992 to 2017. *Ecological Research*, *34*(1), 30. https://doi.org/10.1111/1440-1703.1266

Niklas, K. J., & Enquist, B. J. (2001). Invariant scaling relationships for interspecific plant biomass production rates and body size. *Proceedings of the National Academy of Sciences of the United States of America*, *98*(5), 2922–2927. https://doi.org/10.1073/pnas.041590298

Niklas, K. J., Midgley, J. J., & Rand, R. H. (2003). Size-dependent species richness: Trends within plant communities and across latitude. *Ecology Letters*, *6*(7), 631–636. https://doi.org/10.1046/j.1461-0248.2003.00473.x

Ohtsuka, T., Akiyama, T., Hashimoto, Y., Inatomi, M., Sakai, T., Jia, S., … Koizumi, H. (2005). Biometric based estimates of net primary production (NPP) in a cool-temperate deciduous forest stand beneath a flux tower. *Agricultural and Forest Meteorology*, *134*(1–4), 27–38. https://doi.org/10.1016/j.agrformet.2005.11.005

Phillips, O. L., Malhi, Y., Higuchi, N., Laurance, W. F., Núnez, P. V., Vásquez, R. M., … Grace, J. (1998). Changes in the carbon balance of tropical forests: Evidence from long-term plots. *Science*, *282*(5388), 439–442.

Poorter, H., Jagodzinski, A. M., Ruiz-Peinado, R., Kuyah, S., Luo, Y., Oleksyn, J., … Sack, L. (2015). How does biomass distribution change with size and differ among species? An analysis for 1200 plant species from five continents. *New Phytologist*, *208*(3), 736–749. https://doi.org/10.1111/nph.13571

Poorter, H., Niklas, K. J., Reich, P. B., Oleksyn, J., Poot, P., & Mommer, L. (2012). Biomass allocation to leaves, stems and roots: Meta-analyses of interspecific variation and environmental control. *New Phytologist*, *193*(1), 30–50. https://doi.org/10.1111/j.1469-8137.2011.03952.x

Poorter, L., Wright, S. J., Paz, H., Ackerly, D. D., Condit, R., Ibarra-Manríquez, G., … Wright, I. J. (2008). Are functional traits good

predictors of demographic rates? Evidence from five neotropical forests. *Ecology*, *89*(7), 1908–1920. https://doi.org/10.1890/07-0207.1

Prado-Junior, J. A., Schiavini, I., Vale, V. S., Arantes, C. S., van der Sande, M. T., Lohbeck, M., & Poorter, L. (2016). Conservative species drive biomass productivity in tropical dry forests. *Journal of Ecology*, *104*(3), 817–827. https://doi.org/10.1111/1365-2745.12543

Price, C. A., Gillooly, J. F., Allen, A. P., Weitz, J. S., & Niklas, K. J. (2010). The metabolic theory of ecology: Prospects and challenges for plant biology. *New Phytologist*, *188*(3), 696–710. https://doi.org/10.1111/j.1469-8137.2010.03442.x

Pullmer, M. (2017). *JAGS Version 4.3.0 user manual*. Retrieved from https://web.sgh.waw.pl/~atoroj/ekonometria_bayesowska/jags_user_manual.pdf

R Core Team. (2017). *R: A language and environment for statistical computing*. Vienna, Austria: R Foundation for Statistical Computing. Retrieved from https://www.R-project.org/

Rees, M., Condit, R., Crawley, M., Pacala, S., & Tilman, D. (2001). Long-term studies of vegetation dynamics. *Science*, *293*(5530), 650–655.

Rüger, N., Comita, L. S., Condit, R., Purves, D., Rosenbaum, B., Visser, M. D., … Wirth, C. (2018). Beyond the fast-slow continuum: Demographic dimensions structuring a tropical tree community. *Ecology Letters*, *21*(7), 1075–1084. https://doi.org/10.1111/ele.12974

Rüger, N., Huth, A., Hubbell, S. P., & Condit, R. (2011). Determinants of mortality across a tropical lowland rainforest community. *Oikos*, *120*(7), 1047–1056. https://doi.org/10.1111/j.1600-0706.2010.19021.x

Sheil, D., & Bongers, F. (2020). Interpreting forest diversity-productivity relationships: Volume values, disturbance histories and alternative inferences. *Forest Ecosystems*, *7*(1), 6. https://doi.org/10.1186/s40663-020-0215-x

Sheil, D., Eastaugh, C. S., Vlam, M., Zuidema, P. A., Groenendijk, P., Sleen, P., … Vanclay, J. (2017). Does biomass growth increase in the largest trees? Flaws, fallacies and alternative analyses. *Functional Ecology*, *31*(3), 568–581. https://doi.org/10.1111/1365-2435.12775

Sheil, D., Salim, A., Chave, J., Vanclay, J., & Hawthorne, W. D. (2006). Illumination–size relationships of 109 coexisting tropical forest tree species. *Journal of Ecology*, *94*(2), 494–507. https://doi.org/10.1111/j.1365-2745.2006.01111.x

Sillett, S. C., Van Pelt, R., Koch, G. W., Ambrose, A. R., Carroll, A. L., Antoine, M. E., & Mifsud, B. M. (2010). Increasing wood production through old age in tall trees. *Forest Ecology and Management*, *259*(5), 976–994. https://doi.org/10.1016/j.foreco.2009.12.003

Slik, J. W. F., Paoli, G., McGuire, K., Amaral, I., Barroso, J., Bastian, M., … Zweifel, N. (2013). Large trees drive forest aboveground biomass variation in moist lowland forests across the tropics. *Global Ecology and Biogeography*, *22*(12), 1261–1271. https://doi.org/10.1111/geb.12092

Stephenson, N. L., Das, A. J., Condit, R., Russo, S. E., Baker, P. J., Beckman, N. G., … Zavala, M. A. (2014). Rate of tree carbon accumulation increases continuously with tree size. *Nature*, *507*(7490), 90. https://doi.org/10.1038/nature12914

Talbot, J., Lewis, S. L., Lopez-Gonzalez, G., Brienen, R. J. W., Monteagudo, A., Baker, T. R., … Phillips, O. L. (2014). Methods to estimate aboveground wood productivity from long-term forest inventory plots. *Forest Ecology and Management*, *320*, 30–38. https://doi.org/10.1016/j.foreco.2014.02.021

Wright, S. J., Kitajima, K., Kraft, N. J. B., Reich, P. B., Wright, I. J., Bunker, D. E., … Zanne, A. E. (2010). Functional traits and the growth-mortality trade-off in tropical trees. *Ecology*, *91*(12), 3664–3674. https://doi.org/10.1890/09-2335.1

Xiao, X., White, E. P., Hooten, M. B., & Durham, S. L. (2011). On the use of log-transformation vs. nonlinear regression for analyzing biological power laws. *Ecology*, *92*(10), 1887–1894.

Zanne, A. E., Lopez-Gonzalez, G., Coomes, D. A., Ilic, J., Jansen, S., Lewis, S. L., & Chave, J. (2009). Global wood density database. *Dryad*. Identifier: http://hdl.handle.net/10255/dryad.235

Zhu, Y., Queenborough, S. A., Condit, R., Hubbell, S. P., Ma, K. P., & Comita, L. S. (2018). Density-dependent survival varies with species life-history strategy in a tropical forest. *Ecology Letters*, *21*(4), 506–515. https://doi.org/10.1111/ele.12915

SUPPORTING INFORMATION

Additional supporting information may be found online in the Supporting Information section.

How to cite this article: Kohyama TS, Potts MD, Kohyama TI, et al. Trade-off between standing biomass and productivity in species-rich tropical forest: Evidence, explanations and implications. *J Ecol*. 2020;00:1–13. https://doi.org/10.1111/1365-2745.13485

Trade-off between standing biomass and productivity in species-rich tropical forest: evidence, explanations and implications

T. S. Kohyama, M. D. Potts, T. I. Kohyama, K. Niiyama, T. L. Yao, S. J. Davies, & D. Sheil

Supporting Information

Table S1. Interspecific correlation coefficient matrix between structure-turnover variables in observed (upper triangular, open cells) and identity-free populations (lower triangular, shaded cells) for log-log linear regression in the Pasoh plot.

ln B	0.877	0.264	–0.492	–0.229	–0.277	–0.242
0.850	ln W_{max}	–0.201	–0.533	–0.324	–0.358	–0.304
0.303	–0.206	ln N	(0.044)	0.209	0.178	0.130
–0.719	–0.873	0.195	ln p	0.397	0.493	0.478
(0.038)	(–0.020)	0.130	(0.093)	ln l	0.300	0.517
–0.256	–0.335	0.173	0.296	(0.069)	ln r	0.570
–0.344	–0.448	0.188	0.375	0.140	0.355	ln m

* Correlation coefficients in parentheses are not significant at 5% level.

Table S2. Estimates of net primary production rate by tree growth, P_{plot}, in the Pasoh plot during 1990 and 2000.

Estimates	P_{plot} (Mg ha^{-1} year^{-1})	%-bias
Instantaneous estimates *		
- Subplot-by-species structured	10.03	-
- Species structured	10.02	–0.1%
- Homogeneity approximation	9.61	–4.2%
Simple estimates *		
- Ingrowth included	8.86	–11.7%
- Threshold mass removed	8.82	–12.1%

* See Kohyama, Kohyama and Sheil (2019) for the detail of production rate estimates.

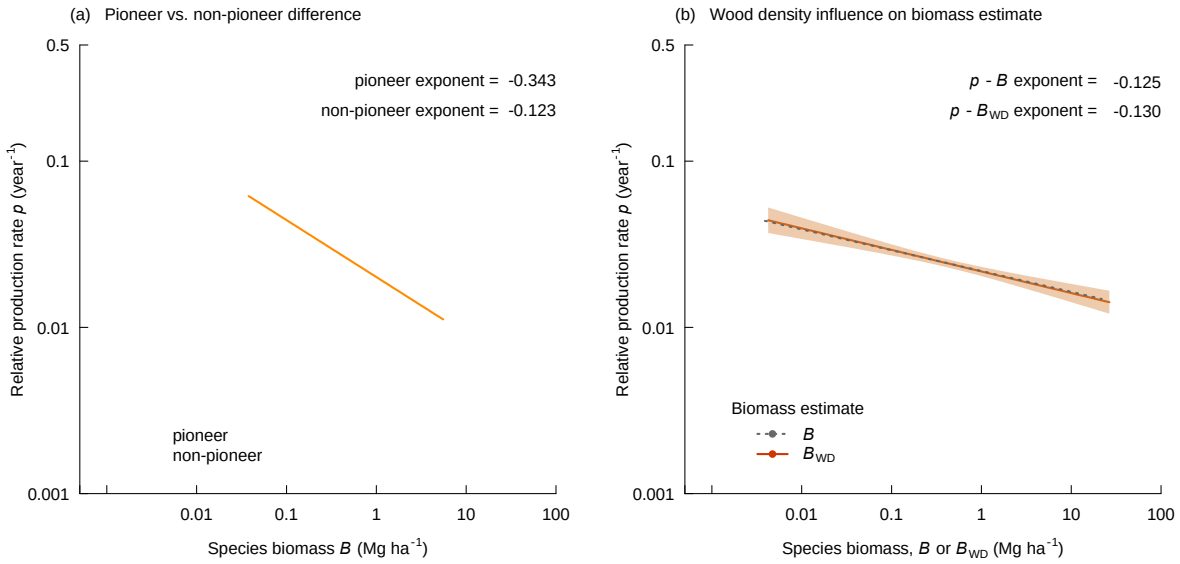

Figure S1. The influence of pioneer species, and the effect of interspecific variation in wood density on the relationship between relative production and biomass among species in the Pasoh plot. (a) Plot of pioneers (orange) versus non-pioneers (blue) among 390 observed species, the two groups were significantly different by AIC model selection. (b) Biomass estimate B with plot-wide common allometry (gray) compared with species-specific biomass estimate B_{WD}, weighted by species-specific wood density ρ (g cm^3) for 210 species that appear both in our 390 species and in Global wood density database (Zanne et al., 2009). Species-specific biomass is $B_{WD} = B_L + \rho(B - B_L)$/[mean ρ for 210 spp.]. Power-function model parameters were not significantly different between p-B and p-B_{WD} model.

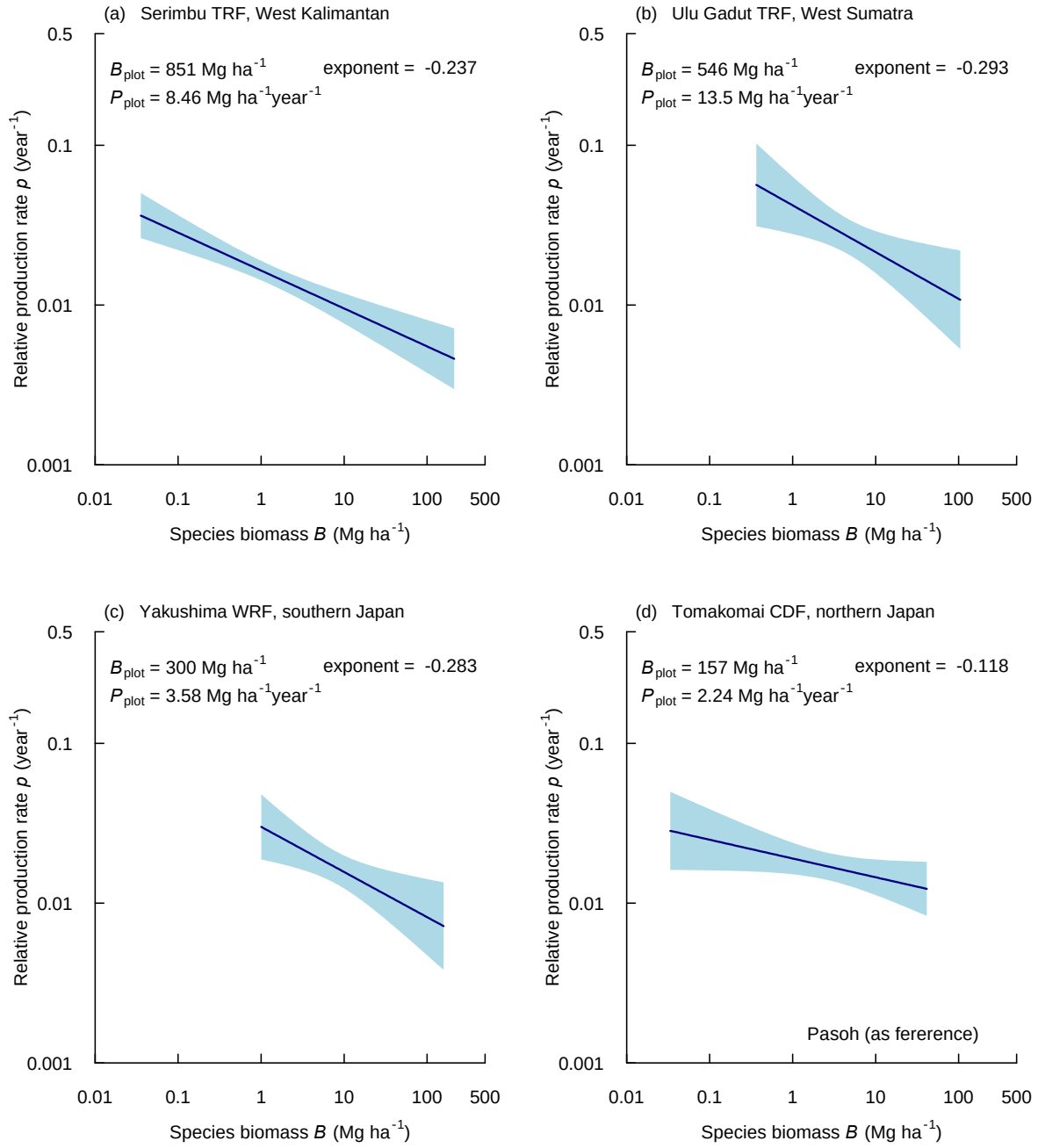

Figure S2. Interspecific relationship of relative productivity on biomass for plots in four old-growth mixed forests. (a) and (b) are tropical rain forests, (c) for warm-temperate evergreen rain forest, and (d) for cool-temperate mixed deciduous broadleaved forest with evergreen conifer *Picea jezoensis*. Blue circles indicate abundant species (≥ 6 survivors), and blue curves with 95% confidence interval show power function fit. Species with the largest biomass were (a) *Dryobalanops beccarii*, (b) *Swintonia schwenkii*, (c) *Distylium racemosum*, and (d) *Acer mono*. Gray dots and lines show the patterns for Pasoh species (≥ 5 cm dbh; ≥ 100 trees). Plot-level biomass B_{plot} and absolute production by tree growth P_{plot} are shown in each panel; those in the Pasoh plot were B_{plot} = 462 Mg ha^{-1} and P_{plot} = 9.88 Mg ha^{-1} year^{-1}.